

Analysis of isotropic tapered beams by using symmetric smoothed particle hydrodynamics method

Armagan Karamanli

Mechatronic Engineering, Faculty of Engineering and Architecture, Istanbul Gelisim University, Avcilar, Istanbul, Turkey

Received: 13 May 2016, Accepted: 18 August 2016

Published online: 29 October 2016.

Abstract: The Symmetric Smoothed Particle Hydrodynamics (SSPH) method is applied to solve elastostatic deformations of isotropic tapered beams subjected to different sets of boundary conditions. Governing equations are presented by using either the Euler-Bernoulli and Timoshenko beam theories. The performance of the SSPH method is evaluated by using different numbers of nodes in the problem domain and employing different beam theories for the numerical solutions of the isotropic tapered beam problems. To validate the performance of the SSPH method, comparison studies in terms of transverse deflections and axial stresses are carried out with the analytical solutions of Euler Bernoulli Beam Theory. Since there is no available closed form solutions of the problems based on the Timoshenko Beam Theory, the analytical solutions obtained by the Euler Beam Theory are used for the comparison purposes. It is observed that the SSPH method has the conventional convergence properties and yields smaller L_2 error.

Keywords: Meshless method, tapered beam, element free, error norm, Timoshenko beam.

1 Introduction

The commonly used beam theories to represent the kinematics of deformation are the Euler Bernoulli Beam Theory (EBT), the Timoshenko Beam Theory (TBT) and the Reddy-Bickford Beam Theory (RBT). The effect of the transverse shear deformation neglected in the EBT is allowed in the latter two beam theories.

The simplest beam theory is the Euler Bernoulli Beam Theory which assumes that the cross sections which are normal to the mid-plane before deformation remain plane/straight and normal to the mid-plane after deformation. By using these assumptions the transverse shear and transverse normal strains can be neglected. The normality assumption of the EBT is relaxed by using the Timoshenko Beam Theory. In the TBT, the cross sections do not need to normal to the mid-plane but still remain plane. The TBT requires the shear correction factor to compensate the error due to the assumption of the constant transverse shear strain and shear stress through the beam thickness, in contrast to the requirement that the upper and lower surfaces of the beam be stress free. The shear correction factor depends on the geometric and material parameters of the beam but the loading and boundary conditions are also important to determine the shear correction factor [1-2]. The third order shear deformation theory which is named as the Reddy-Bickford Beam Theory does not require a shear correction factor due to the fact that through the thickness of the beam the transverse shear strain is quadratic [3].

The need for the further extension of the Euler Bernoulli beam theory is raised for the engineering applications of the beam problems often characterized by high ratios, up to 40 for the composite structures, between the Young modulus and the shear modulus [4]. Various higher order beam theories are introduced in which the straightness assumption is removed and the vanishing of shear stress at the upper and lower surfaces are accommodated. For this purpose, higher order polynomials incorporating either one, or more, extra terms [5-11] or trigonometric functions [12-13] or exponential

* Corresponding author e-mail: afkaramanli@gelisim.edu.tr

functions [14] are included in the expansion of the longitudinal point-wise displacement component through the thickness of the beam. The higher order theories introduce additional unknowns that make the governing equations more complicated and provide the solutions much costly in terms of CPU time.

Meshless methods are widely used in static and dynamic analyses of the engineering beam problems [15-20]. To obtain the approximate solution of the problem by a meshless method, the selection of the basis functions is almost the most important issue. The accuracy of the computed solution can be increased by employing different number of terms in TSE or increasing number of nodes in the problem domain or by increasing the degree of complete polynomials. Many meshless methods have been proposed by researchers to obtain the approximate solution of the problem. The Smoothed Particle Hydrodynamics (SPH) method is proposed by Lucy [21] to the testing of the fission hypothesis. However, this method has two important shortcomings, lack of accuracy on the boundaries and the tensile instability. To remove these shortcomings, many meshless methods have been proposed such as the Corrected Smoothed Particle Method [22,23], Reproducing Kernel Particle Method [24-26], Modified Smoothed Particle Hydrodynamics (MSPH) method [27-30], the Symmetric Smoothed Particle Hydrodynamics method [31-36] and the Strong Form Meshless Implementation of Taylor Series Method [37-38], Moving Kringing Interpolation Method [39-40], the meshless Shepard and Least Squares (MSLS) Method [42], Spectral Meshless Radial Point Interpolation (SMRPI) Method [42].

It is seen from the above literature survey regarding to the SSPH method, there is no reported work on the elastostatic analysis of the isotropic tapered beams subjected to the different boundary conditions by employing the TBT.

The SSPH method has been successfully applied to 2D homogeneous elastic problems including quasi-static crack propagation [31-33], crack propagation in an adhesively bonded joint [34], 2D Heat Transfer problems [35] and 1D fourth order non-homogeneous variable coefficient linear boundary value problems [36].

The SSPH method has an advantage over the MLS, RKPM, MSPH and the SMITSM methods because basis functions used to approximate the function and its derivatives are derived simultaneously, and do not involve derivatives of the weight function that allows to employ a constant weight function [31-36].

In view of the above, the objectives of this paper mainly are to present the SSPH method formulation for the isotropic tapered beams subjected to different boundary conditions within the framework of Euler-Bernoulli Beam Theory and Timoshenko Beam Theory to perform numerical calculations to obtain the transverse deflections and axial stresses of the studied beam problems and finally to compare the results obtained by using the SSPH method with analytical solutions. It is believed that researchers will probably find the SSPH method helpful to solve their engineering problems.

In section 2, the formulation of the EBT and TBT is given. In section 3, the formulation of the SSPH method is presented for 1D problem. In Section 4, numerical results are given based on the two types of engineering beam problem which are a simply supported tapered beam subjected to the uniformly distributed load and a cantilever tapered beam subjected to the uniformly distributed load.

2 Formulation of beam theories

To describe the EBT and TBT the following coordinate system is introduced. The x-coordinate is taken along the axis of the beam and the z-coordinate is taken through the height (thickness) of the beam. In the general beam theory, all the loads and the displacements (u,w) along the coordinates (x,z) are only the functions of the x and z coordinates. [4] The formulation of the EBT and TBT are given below.

2.1 Euler Bernoulli beam theory

The following displacement field is given for the Euler Bernoulli Beam Theory,

$$u(x, z) = -z \frac{dw}{dx}$$

$$w(x, z) = w_0(x) \quad (1)$$

where w_0 is the transverse deflection of the point $(x, 0)$ which is on the mid-plane ($z=0$) of the beam. By using the assumption of the smallness of strains and rotations, the only the axial strain which is nonzero is given by,

$$\varepsilon_{xx} = \frac{du}{dx} = -z \frac{d^2 w_0}{dx^2}. \quad (2)$$

The virtual strain energy of the beam in terms of the axial stress and the axial strain can be expressed by

$$\delta U = \int_0^L \int_A \sigma_{xx} \delta \varepsilon_{xx} dA dx \quad (3)$$

where δ is the variational symbol, A is the cross sectional area of the non-uniform beam, L is the length of the beam, σ_{xx} is the axial stress. The bending moment of the EBT is given by,

$$M_{xx} = \int_A z \sigma_{xx} dA. \quad (4)$$

By using Equation (2) and Equation (4), Equation (3) can be rewritten as,

$$\delta U = - \int_0^L M_{xx} z \frac{d^2 \delta w_0}{dx^2} dx. \quad (5)$$

The virtual potential energy of the load $q(x)$ which acts at the centroidal axis of the beam is given by

$$\delta V = - \int_0^L q(x) \delta w_0 dx. \quad (6)$$

If a body is in equilibrium, $\delta W = \delta U + \delta V$, the total virtual work (δW) done is zero. Then one can obtain,

$$\delta W = - \int_0^L \left(M_{xx} z \frac{d^2 \delta w_0}{dx^2} + q(x) \delta w_0 \right) dx = 0. \quad (7)$$

After performing integration by parts of the first term in Equation (2.7) twice and since δw_0 is arbitrary in $(0 < x < L)$, one can obtain following equilibrium equation

$$- \frac{d^2 M_{xx}}{dx^2} = q(x), \text{ for } 0 < x < L. \quad (8)$$

By introducing the shear force Q_x and rewrite the Equation (2.8) in the following form

$$- \frac{dM_{xx}}{dx} + Q_x = 0,$$

$$- \frac{dQ_x}{dx} = q(x). \quad (9)$$

By using Hooke's law, one can obtain

$$\sigma_{xx} = E\varepsilon_{xx} = -Ez \frac{d^2 w_0}{dx^2} \quad (10)$$

where E is the modulus of elasticity. If the Equation (10) is put into the Equation (4), it is obtained,

$$M_{xx} = - \int_A Ez^2 \frac{d^2 w_0}{dx^2} dA = -D_{xx} \frac{d^2 w_0}{dx^2} \quad (11)$$

where $D_{xx} = EI_y$ is the flexural rigidity of the beam and $I_y = \int_A z^2 dA$ the second moment of area about the y-axis. The substitution of Equation (2.11) into Equation (2.9) yields the Euler Bernoulli Beam Theory governing equation

$$\frac{d^2}{dx^2} (D_{xx} \frac{d^2 w_0}{dx^2}) = q(x), \text{ for } 0 < x < L. \quad (12)$$

2.2 Timoshenko beam theory

The following displacement field is given for the Timoshenko Beam Theory,

$$u(x, z) = z\phi(x),$$

$$w(x, z) = w_0(x) \quad (13)$$

where $\phi(x)$ denotes the rotation of the cross section. By using the Equation (13), the strain-displacement relations are given by

$$\varepsilon_{xx} = \frac{du}{dx} = -z \frac{d\phi}{dx}$$

$$\gamma_{xz} = \frac{du}{dz} + \frac{dw}{dx} = \phi + \frac{dw_0}{dx}. \quad (14)$$

The virtual strain energy of the beam including the virtual energy associated with the shearing strain can be written as,

$$\delta U = \int_0^L \int_A (\sigma_{xx} \delta \varepsilon_{xx} + \sigma_{xz} \delta \gamma_{xz}) dA dx \quad (15)$$

where σ_{xz} is the transverse shear stress and γ_{xz} is the shear strain. The bending moment and the shear force can be written respectively

$$M_{xx} = \int_A z \sigma_{xx} dA, Q_x = \int_A \sigma_{xz} dA. \quad (16)$$

By using Equation (14) and Equation (16), one can rewrite the Equation (15) as,

$$\delta U = \int_0^L \left[M_{xx} \frac{d\delta\phi}{dx} + Q_x \left(\delta\phi + \frac{d\delta w_0}{dx} \right) \right] dx. \quad (17)$$

The virtual potential energy of the load $q(x)$ which acts at the centroidal axis of the Timoshenko beam is given by

$$\delta V = - \int_0^L q(x) \delta w_0 dx. \quad (18)$$

Since the total virtual work done is zero and the coefficients of $\delta\phi$ and δw_0 in $0 < x < L$ are zero, one can obtain the following equilibrium equations

$$\begin{aligned} -\frac{dM_{xx}}{dx} + Q_x &= 0, \\ -\frac{dQ_x}{dx} &= q(x). \end{aligned} \tag{19}$$

The bending moment and shear force can be expressed in terms of generalized displacement (w_0, ϕ) by using the constitutive equations $\sigma_{xx} = E\varepsilon_{xx}$ and $\sigma_{xz} = G\gamma_{xz}$,

$$M_{xx} = \int_A z\sigma_{xx}dA = D_x \frac{d\phi}{dx} \tag{20}$$

$$Q_x = \kappa_s \int_A \sigma_{xz}dA = \kappa_s A_{xz} \left(\phi + \frac{dw_0}{dx} \right) \tag{21}$$

where κ_s is the shear correction factor, G is the shear modulus, $D_{xx} = EI_y$ is the flexural rigidity of the beam and $A_{xz} = GA$ is the shear rigidity. The shear correction factor is used to compensate the error caused by assuming a constant transverse shear stress distribution through the beam depth.

The governing equations of the Timoshenko Beam Theory is obtained in terms of generalized displacements by substituting the Equations (20) and Equation (21) into Equation (19),

$$-\frac{d}{dx} \left(D_{xx} \frac{d\phi}{dx} \right) + \kappa_s A_{xz} \left(\phi + \frac{dw_0}{dx} \right) = 0 \tag{22}$$

$$-\frac{d}{dx} \left[\kappa_s A_{xz} \left(\phi + \frac{dw_0}{dx} \right) \right] = q(x). \tag{23}$$

3 Formulation of symmetric smoothed particle hydrodynamics

The governing Taylor Series Expansion (TSE) of a scalar function can be given by

$$f(\xi_1) = \sum_{m=0}^n \frac{1}{m!} \left[(\xi_1 - x_1) \frac{d}{dx_1} \right]^m f(x_1) \tag{24}$$

where $f(\xi_1)$ is the value of the function at $\xi = (\xi_1)$ located in near of $x = (x_1)$. If the zeroth to fourth order terms are employed and the higher order terms are neglected, the Equation (24) can be written as follows

$$f(\xi) = P(\xi, x)R(x) \tag{25}$$

where

$$R(x) = \left[f(x), \frac{df(x)}{dx_1}, \frac{1}{2!} \frac{d^2f(x)}{dx_1^2}, \dots, \frac{1}{4!} \frac{d^4f(x)}{dx_1^4} \right]^T \tag{26}$$

$$P(\xi, x) = \left[1, (\xi_1 - x_1), (\xi_1 - x_1)^2, \dots, (\xi_1 - x_1)^4 \right] \tag{27}$$

To determine the unknown variables given in the $R(x)$, both sides of Equation (??) are multiplied with $W(\xi, x)P(\xi, x)^T$ and evaluated for every node in the CSD. The following equation is obtained

$$\sum_{j=1}^{N(x)} f(\xi^{r(j)}) W(\xi^{r(j)}, x) P(\xi^{r(j)}, x)^T$$

$$\sum_{j=1}^{N(x)} \left[P(\xi^{r(j)}, x)^T W(\xi^{r(j)}, x) P(\xi^{r(j)}, x) \right] R(x) \tag{28}$$

where $N(x)$ is the number nodes in the compact support domain (CSD) of the $W(\xi, x)$ as shown in Figure 1. Then,

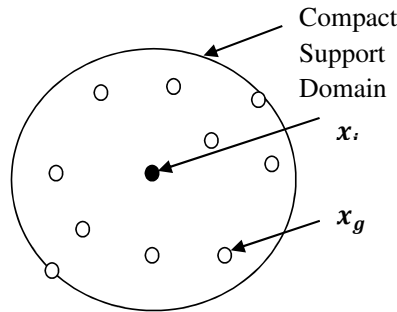


Fig. 1: Compact support of the weight function $W(\xi, x)$ for the node located at $x = (x_i, y_i)$

equation (28) can be given by

$$C(\xi, x)R(x) = H(\xi, x)F^{(x)}(\xi, x) \tag{29}$$

where $C(\xi, x) = P(\xi, x)^T W(\xi, x) P(\xi, x)$ and $H(\xi, x) = P(\xi, x)^T W(\xi, x)$. The solution of Equation (29) is given by

$$R(x) = K(\xi, x)F^{(x)}(\xi) \tag{30}$$

where $K^{(x)}(\xi, x) = C(\xi, x)^{-1}H(\xi, x)$ and $F^{(x)T}(\xi) = [f(\xi^{r(1)}), f(\xi^{r(2)}), \dots, f(\xi^{r(N(x))})]$. Equation (30) can be also written as follows

$$R_I(x) = \sum_{J=1}^M K_{IJ}F_J, I = 1, 2, \dots, 5, \tag{31}$$

where M is the number of nodes and $F_J = f(\xi^J)$. Five components of Equation (31) for 1D case are can be written as

$$f(x) = R_1(x) = \sum_{J=1}^M K_{1J}F_J$$

$$\frac{df(x)}{dx_1} = R_2(x) = \sum_{J=1}^M K_{2J}F_J$$

$$\frac{d^2f(x)}{dx_1^2} = 2!R_3(x) = \sum_{J=1}^M K_{3J}F_J$$

$$\frac{d^3 f(x)}{dx_1^3} = 3!R_4(x) = \sum_{J=1}^M K_{4J}F_J$$

$$\frac{d^4 f(x)}{dx_1^4} = 4!R_5(x) = \sum_{J=1}^M K_{5J}F_J. \tag{32}$$

The formulation for 2D and 3D problems can be found [31-34].

4 Numerical results

The SSPH method is applied to solve the pure bending of two engineering tapered beam problems by using the formulation of the EBT and TBT. Different loading and boundary conditions are applied with different node distributions in the problem domain. The numerical results obtained by the SSPH method are compared with the analytical solution of problem obtained by the EBT. For both problems, the analytical solutions based on the TBT are not available in closed form. So that, the comparisons for the numerical solutions obtained by the TBT are carried out by using the analytical solutions based on the EBT. We assume that there is no lateral buckling.

4.1 Simply supported beam

To determine the static transverse deflections, axial stresses and transverse shear stress of a simply supported tapered beam under uniformly distributed load of intensity q_0 is considered as shown in Fig.2. is studied.

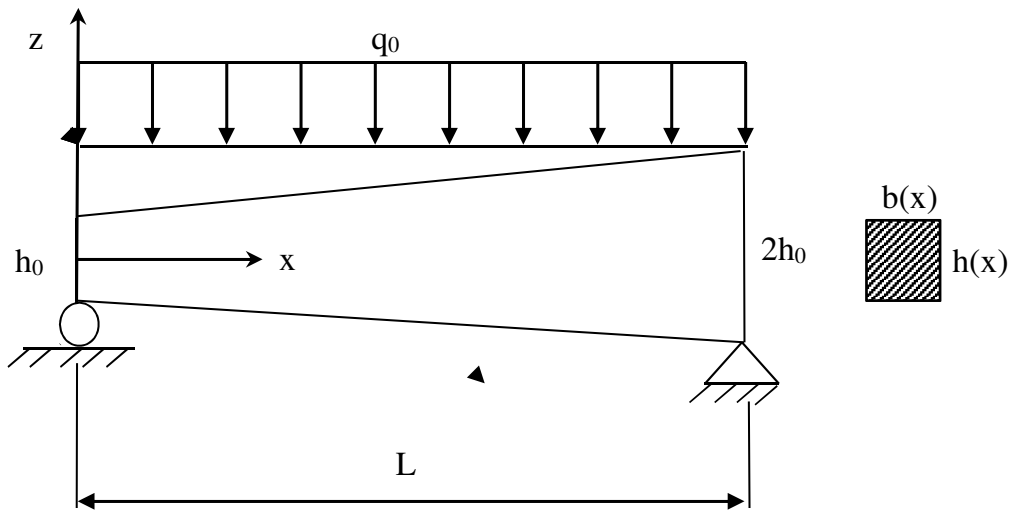


Fig. 2: Simply Supported Beam with Uniformly Distributed Load.

The width b and depth h of the tapered beam are varying linearly along the x -direction

$$b = b_0 \left(1 + \frac{x}{L}\right), \quad h = h_0 \left(1 + \frac{x}{L}\right)$$

where b_0 is the width of the beam cross section at $x = 0$, h_0 is the depth of the beam cross section at $x = 0$ and L is the length of the beam.

The physical parameters of the beam are given as $L=2m$, $h_0=0.1m$, $b_0=0.01m$. Modulus of elasticity E is 210 GPa, shear modulus G is 80.8 GPa and the distributed load q_0 is set to $50000N/m$.

Based on the EBT, the governing equation of the problem can be given by,

$$\frac{d^2}{dx^2}(D_{xx}(x)\frac{d^2w_0}{dx^2}) = q_0, \text{ for } 0 < x < L \tag{33}$$

where $D_{xx}(x) = EI_y(x)$ is the flexural rigidity of the beam and $I_y(x) = (b_0h_0^3/12)(1 + x/L)^4$ is the second moment of area about the y-axis. The boundary conditions regarding to the EBT are given as follows;

$$x = 0, \quad \frac{d^2w_0}{dx^2} = 0 \text{ and } w_0 = 0 \text{ m}$$

$$x = L, \quad \frac{d^2w_0}{dx^2} = 0 \text{ and } w_0 = 0 \text{ m.}$$

The analytical solution of this problem obtained by using MATLAB is given by

$$w_0^E(x) = \frac{\left[\lambda + 16\lambda (0.5 \ln(2) - 0.3125) (0.25x^2 + x + 1)^{\frac{1}{2}} \right] + 4 \left[8\lambda \left[\left(0.5 \ln(x+2) - 0.5 \ln(2) + \left(\frac{2x+3}{(x+2)^2} \right) - 0.75 \right) + 16\lambda \left[\frac{(x+1)(x^2+4x+4)^{\frac{1}{2}}}{2(x+2)^3 - 0.125} \right] \right] \right] (0.25x^2 + x + 1)^{\frac{1}{2}}}{x + 2} \tag{34}$$

where the superscript E denotes the quantities in the EBT, $\lambda = \frac{12q_0}{Eb_0h_0^3}$.

The governing equations of the problem can be written by using TBT as follows,

$$-\frac{d}{dx} \left(D_{xx} \frac{d\phi}{dx} \right) + \kappa_s A_{xz} \left(\phi + \frac{dw_0}{dx} \right) = 0 \tag{35}$$

$$-\frac{d}{dx} \left[\kappa_s A_{xz} \left(\phi + \frac{dw_0}{dx} \right) \right] = q_0 \tag{36}$$

where $A_{xz}(x) = GA(x) = Gb_0h_0(1 + x/L)^2$ is the shear rigidity and the shear correction factor is assumed to be constant $\kappa_s = 5/6$ for the rectangular cross section.

The boundary conditions regarding to the TBT are given as follows;

$$x = 0, \quad \frac{d\phi}{dx} = 0 \text{ and } w_0 = 0 \text{ m}$$

$$x = L, \quad \frac{d\phi}{dx} = 0 \text{ and } w_0 = 0 \text{ m.}$$

The analytical solution of this boundary value problem is not available in the literature with the explicit form and could not be obtained by using MATLAB.

The above boundary value problems are solved by using the SSPH method for the node distributions of 21, 41 and 161 equally spaced nodes in the domain $x \in [0, 2]$. The following Revised Super Gauss Function in [31] is used as the weight

function since it resulted in the least L_2 error norms in numerical solutions presented in [31].

$$W(x, \xi) = \frac{G}{(h\sqrt{\pi})^\lambda} \begin{cases} (25 - d^2) e^{-d^2} & 0 \leq d \leq 5 \\ 0 & d > 5 \end{cases} \quad (37)$$

where $d = |x - \xi|/\rho$ is the radius of the support domain, h is the smoothing length.

The numerical solutions are performed according to the following meshless parameters; the radius of the support domain (d) is chosen as 5 and the smoothing length (ρ) equals to Δ where Δ is the minimum distance between two adjacent nodes. The parameter values of d and h are selected that yield the best accuracy.

Numerical results obtained by using the SSPH method are compared with the analytical solutions, and their convergence and accuracy features are evaluated by using the following global L_2 error norm,

$$L_2 = \frac{\left[\sum_{j=1}^m (v_{num}^j - v_{exact}^j)^2 \right]^{1/2}}{\left[\sum_{j=1}^m (v_{exact}^j)^2 \right]^{1/2}} \quad (38)$$

where v_{num}^j is the value of numerical solution at the j^{th} node and v_{exact}^j is the value of analytical solution at the j^{th} node.

The global L_2 error norms of the numerical solutions in terms of transverse deflections based on the EBT are given in Table 1. For the numerical analysis different numbers of nodes are considered in the problem domain with 5 terms in TSEs expansion. The numerical results in Table 1 are obtained for the parameter values of d and ρ giving the best accuracy for each method. It is observed in Table 1 that the accuracy of the SSPH method increases when the number of nodes in the problem domain increases. The convergence rate of the SSPH method increases with an increase in the number of nodes.

It is observed in Figure 3 that the SSPH method agrees very well with the analytical solution. The transverse deflection of the beam computed by the SSPH method is virtually indistinguishable from that for the analytical solution for the 161 uniform of location of nodes in the problem domain.

Table 1: Global L_2 error norm in terms of transverse displacements for different number of nodes based on the EBT.

Meshless Method	Number of Nodes		
	21 Nodes	41 Nodes	161 Nodes
SSPH	1.4151	0.2378	0.0049

The global L_2 error norms of the numerical solutions in terms of axial stress based on the EBT are given in Table 2. It is observed in Table 2 that the 161 uniform of location of nodes in the problem domain gives the least error in the numerical solution. For each of the numerical solutions, the maximum difference in the computed and analytical values of axial stress decreases with an increase in the number of nodes. Figure 4 exhibits the computed axial stress at $x=0$ for uniform node placements of 21, 41 and 161. The results are much closer to the analytical solution compared to those given by 161 nodes.

The numerical solutions obtained by using TBT are compared with the analytical solution of the problem computed by using EBT. It is observed in Figure 5 that the computed transverse deflections along the beam by using TBT are higher than the analytical solution of the EBT. As it is very well known that the inclusion of the shear deformation in Timoshenko beam theory makes the beam more flexible which results in higher transverse deflections.

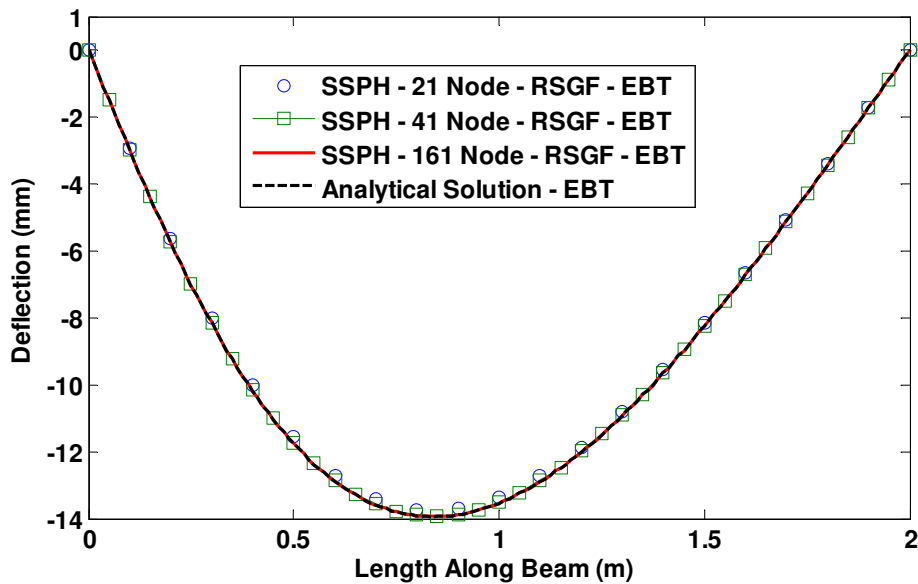


Fig. 3: Transverse deflections of the beam based on the EBT along the x -axis computed by the SSPH method using different number of nodes and the analytical solution.

Table 2: Global L_2 error norm in terms of axial stress for different number of nodes based on the EBT.

Meshless Method	Number of Nodes		
	21 Nodes	41 Nodes	161 Nodes
SSPH	0.9779	0.1754	0.0050

In Figure 6, the axial stresses computed by the TBT are given. The difference between the axial stresses of EBT and TBT is negligible at least for the problem studies here.

In Table 3, the transverse shear stresses computed by the SSPH method based on the TBT are given. With an increase in the number of nodes, the computed transverse shear stress value decreases.

Table 3: Transverse shear stress (MPa) for different number of nodes based on TBT.

Meshless Method	Number of Nodes		
	21 Nodes	41 Nodes	161 Nodes
SSPH	-67.4598	-60.7852	-60.0044

4.2 Cantilever beam

For a cantilever tapered beam the static transverse deflections under uniformly distributed load of intensity q_0 as shown in Figure 7 is studied.

The width b and depth h of the tapered beam are varying linearly along the x -direction,

$$b = b_0 \left(1 + \frac{x}{L}\right), \quad h = h_0 \left(1 + \frac{x}{L}\right)$$

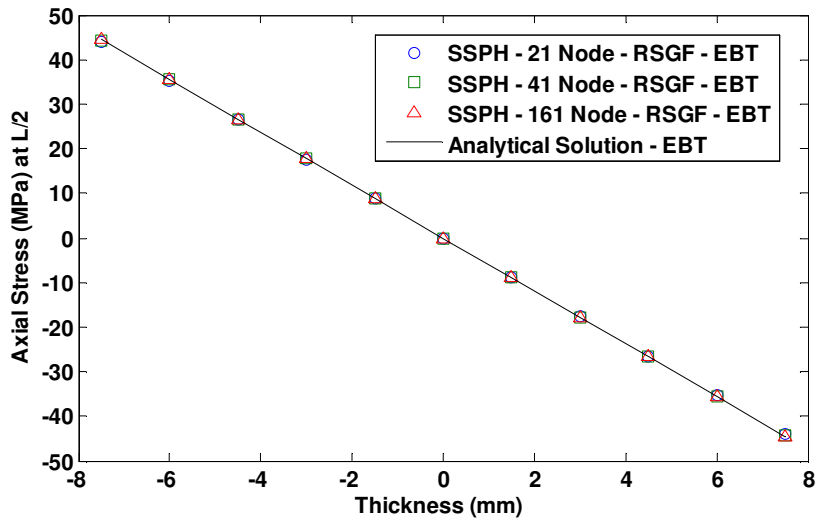


Fig. 4: Axial stresses of the beam at $x=L/2$ along the thickness of the beam computed by the SSPH method using different number of nodes and the analytical solution.

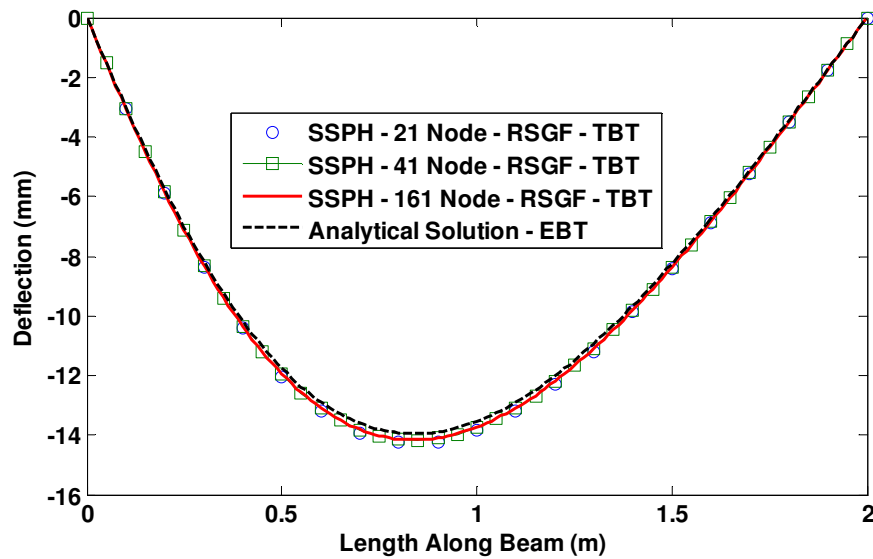


Fig. 5: Transverse deflections of the beam based on the TBT and the analytical solution.

where b_0 is the width of the beam cross section at $x=0$, h_0 is the depth of the beam cross section at $x=0$ and L is the length of the beam.

The physical and material parameters and of the beam are same with the previous example, as well as the load.

Based on the EBT, the governing equation of the problem is as given in Equation (33). The boundary conditions are given by;

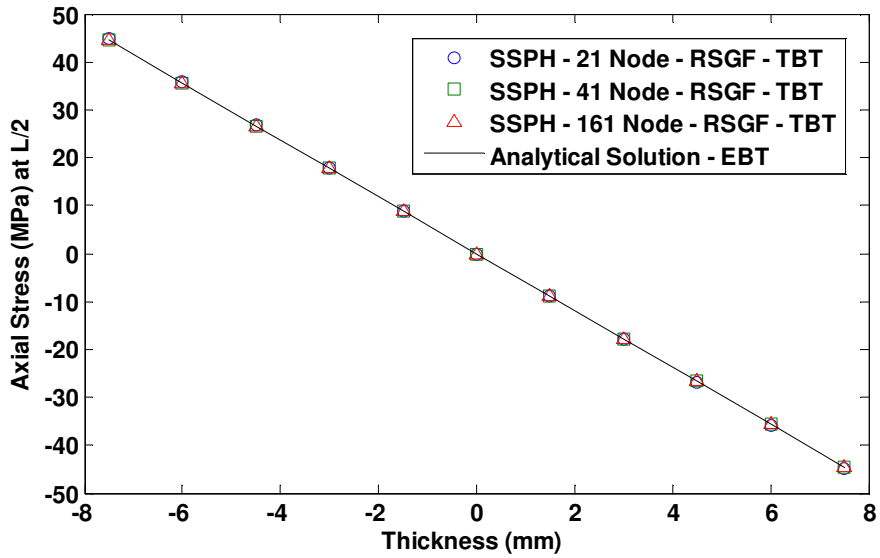


Fig. 6: Axial stresses of the beam at $x = L/2$ along the thickness of the beam computed by the SSPH method using different number of nodes and the analytical solution.

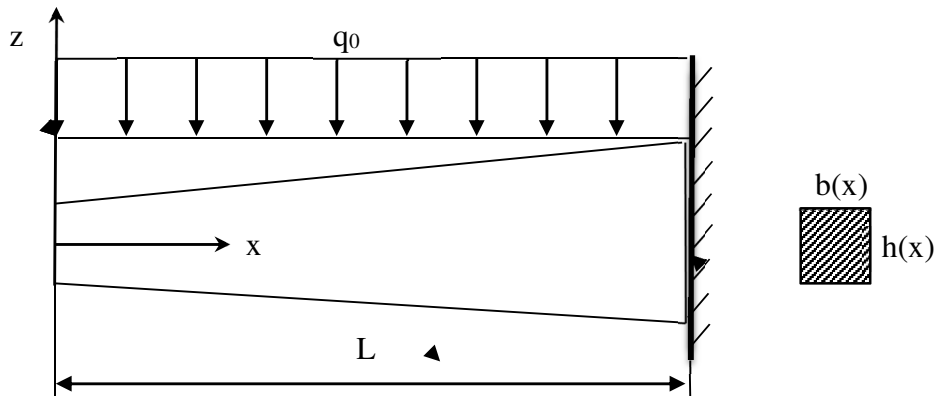


Fig. 7: Cantilever beam with uniformly distributed load.

$$x = L, \quad \frac{dw_0}{dx} = 0 \text{ and } w_0 = 0 \text{ m,}$$

$$x = 0, \quad \frac{d^2w_0}{dx^2} = 0 \text{ and } \frac{d^3w_0}{dx^3} = 0.$$

The analytical solution of this boundary value problem based on the EBT is given by

$$w_0^E(x) = \left[\frac{7\lambda(0.25x^2 + x + 1)^{\frac{1}{2}}}{3} \right] - \frac{16 \left[(0.25x^2 + x + 1)^{\frac{1}{2}} + (x^2 + 4x + 4)^{\frac{1}{2}} (3\lambda x^2 + 6\lambda x + 4\lambda) \right]}{3(x+2)^4} - \frac{32\lambda \left[(x^2 + x + 1)^{\frac{1}{2}} \left(0.5 \ln(x+2) - \ln(2) + \left(\frac{2x+3}{(x+2)^2} \right) - \frac{7}{16} \right) \right]}{(x+2)} \tag{39}$$

Based on the TBT, the governing equations of the problem are given in Equation (35) and Equation (36). The boundary conditions regarding to the TBT are given as follows;

$$x = L, \quad \phi = 0 \text{ and } w_0 = 0 \text{ m,}$$

$$x = 0, \quad \frac{d\phi}{dx} = 0 \text{ and } \phi + \frac{dw_0}{dx} = 0.$$

The analytical solution of this boundary value problem is not available in the literature with the explicit form and could not be obtained by using MATLAB.

The above boundary value problems are solved by using the SSPH method for the node distributions of 21, 41 and 161 equally spaced nodes in the domain $x \in [0,2]$. The Revised Super Gauss Function given in Equation (??) is used as the weight function. For the numerical solutions, the radius of the support domain (d) is chosen as 5 and the smoothing length (ρ) is chosen as Δ . The parameter values of d and ρ are selected that yield the best accuracy.

Numerical results obtained by using the SSPH method are compared with the analytical solutions, and their convergence and accuracy features are evaluated by using the global L_2 error norm given in Equation (38). In Table 4 the global L_2 error norms of the solutions based on the EBT are given for different numbers of nodes in the problem domain with 5 terms in TSEs expansion.

Table 4: Global L_2 error norm for different number of nodes based on EBT.

Meshless Method	Number of Nodes		
	21 Nodes	41 Nodes	161 Nodes
SSPH	7.9056	2.5793	0.2022

The accuracy of the SSPH method increases by increasing of the number of nodes in the problem domain. The computed transverse deflection of the beam is virtually indistinguishable from that for the analytical solution. The SSPH method agrees very well with the analytical solution as seen from Figure 8.

The global L_2 error norms of the numerical solutions in terms of axial stress based on the EBT are given in Table 5. It is observed in Table 2 that for each of the numerical solutions, the maximum difference in the computed and analytical values of axial stress decreases with an increase in the number of nodes. Figure 9 exhibits the computed axial stress at $x = 0$ for uniform node placements of 21, 41 and 161. The results are much closer to the analytical solution compared to those given by 161 nodes.

The numerical solutions obtained by using TBT are compared with the analytical solution of the problem computed by using EBT. It is observed in Figure 10 that the computed transverse deflections along the beam by using TBT are higher than the analytical solution of the EBT. As stated earlier that the inclusion of the shear deformation in Timoshenko

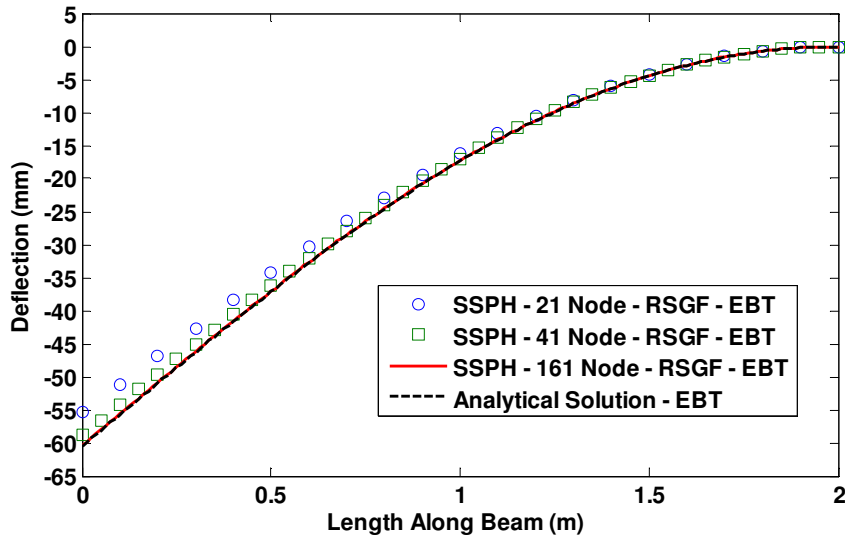


Fig. 8: Transverse deflections of the beam based on the EBT along the x-axis computed by the SSPH method using different number of nodes and the analytical solution.

Table 5: Global L_2 error norm in terms of axial stress for different number of nodes based on the EBT.

Meshless Method	Number of Nodes		
	21 Nodes	41 Nodes	161 Nodes
SSPH	5.6540	1.8236	0.1419

beam theory makes the beam more flexible which results in higher transverse deflections. In Figure 11, the axial stresses computed by the TBT are given. The difference between the axial stresses of EBT and TBT is very small at least for the problem studies here.

Table 6: Transverse shear stress (MPa) for different number of nodes based on TBT.

Meshless Method	Number of Nodes		
	21 Nodes	41 Nodes	161 Nodes
SSPH	30.4648	30.0547	30.0003

The transverse shear stresses computed by the SSPH method based on the TBT are given in Table 6. It is observed that with an increase in the number of nodes, the computed transverse shear stress value decreases.

5 Conclusion

The SSPH basis functions are employed to numerically solve the elastostatic analysis of the isotropic tapered beams subjected to different sets of boundary conditions and uniformly distributed load by using strong formulation of the problem. The numerical calculations are performed by using different number of nodes uniformly distributed in the problem domain and by employing different beam theories which are the EBT and TBT. The performance of the SSPH method is investigated for the solution of the tapered beam problems with the TBT for the first time. It is found that the SSPH method provides satisfactory results and convergence rate for the studied problems here. It is observed that the

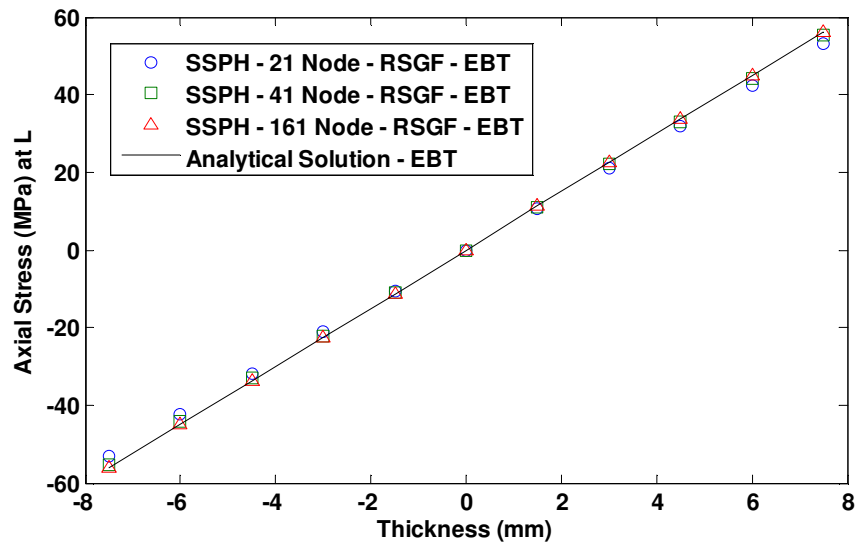


Fig. 9: Axial stresses of the beam at $x = L$ along the thickness of the beam computed by the SSPH method using different number of nodes and the analytical solution.

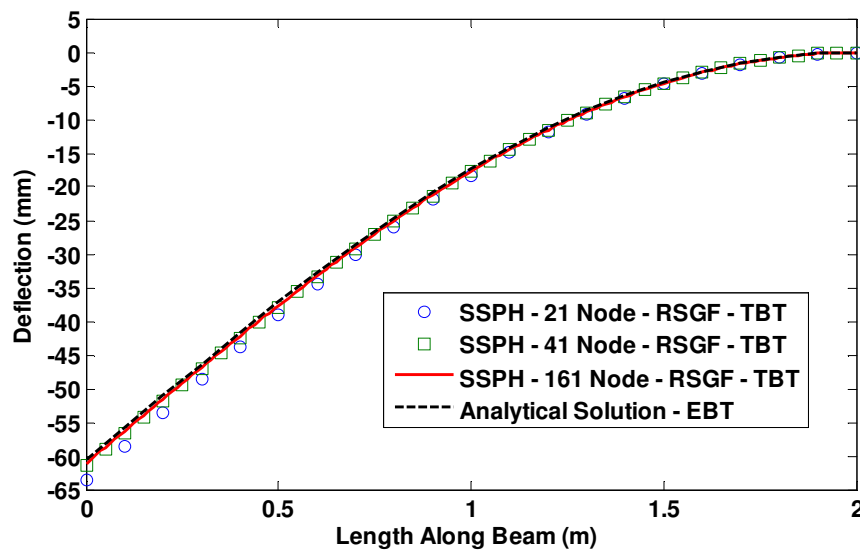


Fig. 10: Transverse deflections of the beam based on the TBT along the x -axis computed by the SSPH method using different number of nodes and the analytical solution.

computed results of transverse deflections and axial stresses agree very well with the analytical solutions and are virtually indistinguishable from that for analytical solution.

Since the analytical solutions of the problems based on the TBT formulation are not available, the computed results are compared with the analytical solutions of EBT formulation. The transverse deflections and the axial stresses obtained by the TBT formulation are found agree well with those obtained from the analytical solution of EBT. Based on the results

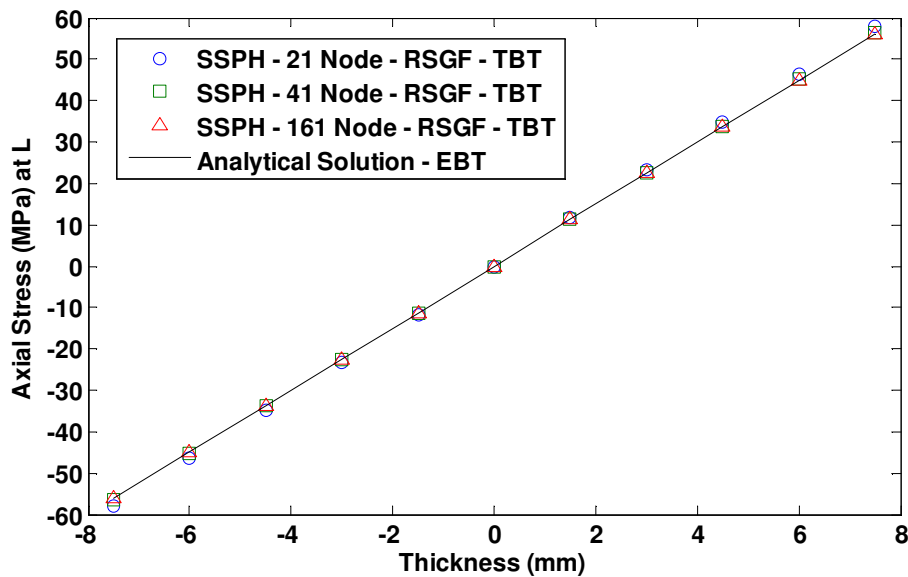


Fig. 11: Axial stresses of the beam at $x = L$ along the thickness of the beam computed by the SSPH method using different number of nodes and the analytical solution.

of two numerical examples it is recommended that the SSPH method can be applied for solving linear beam problems with varying cross sections by employing the TBT formulation.

Competing interests

The authors declare that they have no competing interests.

Authors' contributions

All authors have contributed to all parts of the article. All authors read and approved the final manuscript.

References

- [1] Love, A.E.H., 1927, A Treatise on the Mathematical Theory of Elasticity, fourth ed. Dover Publications, New York.
- [2] Timoshenko, S.P., Goodier, J.C., 1970, Theory of Elasticity, McGraw-Hill Co. Inc., New York.
- [3] Wang, C.M., Reddy, J.N., Lee, K.H., 2000, Shear Deformable Beams and Plates Relations with Classical Solutions, Elsevier Science Ltd., Oxford.
- [4] Polizzotto, C., 2015, From the Euler-Bernoulli beam to the Timoshenko one through a sequence of Reddy-type shear deformable beam models of increasing order, European Journal of Mechanics A/Solids, 53, 62-74.
- [5] Levinson, M., 1981. A new rectangular beam theory, Journal of Sound and Vibration, 74, 81-87.
- [6] Bickford, W.B., 1982. A consistent higher order beam theory, Theor. Appl. Mech. 11, 137-150.
- [7] Heyliger, P.R., Reddy, J.N., 1988, A higher order beam finite element for bending and vibration problems, Journal of Sound and Vibration, 126 (2), 309-326.
- [8] Subramanian, P., 2006, Dynamic analysis of laminated composite beams using higher order theories and finite elements, Composite Structures, 73, 342-353.

- [9] Reddy, J.N., 2007, Nonlocal theories for bending, buckling and vibration of beams, *Int. J. Eng. Sci.* 45, 288-307.
- [10] Carrera, E., Giunta, G., 2010, Refined beam theories based on a unified formulation, *Int. J. Appl. Mech.* 2 (1), 117-143.
- [11] Giunta, G., Biscani, F., Bellouettar, S., Ferreira, A.J.M., Carrera, E., 2013, Free vibration analysis of composite beams via refined theories, *Composites Part B*, 44, 540-552.
- [12] Arya, H., 2003, A new zig-zag model for laminated composite beams: free vibration analysis, *Journal of Sound and Vibration*, 264, 485-490.
- [13] Jun, L., Hongxing, H., 2009, Dynamic stiffness analysis of laminated composite beams using trigonometric shear deformation theory, *Composite Structures*, 89, 433-442.
- [14] Kurama, M., Afaq, K.S., Mistou, S., 2003, Mechanical behavior of laminated composite beams by the new multi-layered laminated composite structures model with trigonometric shear stress continuity, *Int. J. Solids Struct.* 40, 1525-1546.
- [15] Donning, B.M., Liu, W.K., 1998, Meshless methods for shear-deformable beams and plates, *Computer Methods in Applied Mechanics and Engineering*, 152, 47-71.
- [16] Gu, Y.T., Liu, G.R., 2001, A local point interpolation method for static and dynamic analysis of thin beams, *Computer Methods in Applied Mechanics and Engineering*, 190,42, 5515-5528.
- [17] Ferreira, A.J.M., Roque, C.M.C., Martins, P.A.L.S., 2004, Radial basis functions and higher-order shear deformation theories in the analysis of laminated composite beams and plates, *Composite Structures*, 66, 287-293.
- [18] Ferreira, A.J.M., Fasshauer, G.E., 2006, Computation of natural frequencies of shear deformable beams and plates by an RBF-pseudospectral method, 196, 134-146.
- [19] Moosavi, M.R., Delfanian, F., Khelil, A., 2011, The orthogonal meshless finite volume method for solving Euler-Bernoulli beam and thin plate problems, 49, 923-932.
- [20] Roque, C.M.C., Figaldo, D.S., Ferreira, A.J.M., Reddy, J.N., 2013, A study of a microstructure-dependent composite laminated Timoshenko beam using a modified couple stress theory and a meshless method, 96, 532-537.
- [21] Lucy LB, A numerical approach to the testing of the fission hypothesis, *Astron J* 82, 1013-1024, 1977.
- [22] Chen JK, Beraun JE, Jin CJ, An improvement for tensile instability in smoothed particle hydrodynamics, *Comput Mech* 23, 279-287, 1999.
- [23] Chen JK, Beraun JE, Jin CJ, Completeness of corrective smoothed particle method for linear elastodynamics, *Comput Mech* 24, 273-285, 1999.
- [24] Liu WK, Jun S, Zhang YF, Reproducing kernel particle methods, *Int J Num Meth Fluids* 20, 1081-1106, 1995.
- [25] Liu WK, Jun S, Li S, Adee J, Belytschko T, Reproducing kernel particle methods for structural dynamics, *Int J Num Meth Eng* 38, 1655-1679, 1995.
- [26] Chen JS, Pan C, Wu CT, Liu WK, Reproducing kernel particle methods for large deformation analysis of non-linear structures, *Comput Method Appl Mech Eng* 139, 195-227, 1996.
- [27] Zhang GM, Batra RC, Modified smoothed particle hydrodynamics method and its application to transient problems, *Comput Mech* 34, 137-146, 2004.
- [28] Batra RC, Zhang GM, Analysis of adiabatic shear bands in elasto-thermo-viscoplastic materials by modified smoothed particle hydrodynamics (MSPH) method, *J Comput Phys* 201, 172-190, 2004.
- [29] Zhang GM, Batra RC, Wave propagation in functionally graded materials by modified smoothed particle hydrodynamics (MSPH) method, *J Comput Phys* 222, 374-390, 2007.
- [30] Batra RC, Zhang GM, Search algorithm, and simulation of elastodynamic crack propagation by modified smoothed particle hydrodynamics (MSPH) method, *Comput Mech* 40, 531-546, 2007.
- [31] Zhang GM, Batra RC, Symmetric smoothed particle hydrodynamics (SSPH) method and its application to elastic problems, *Comput Mech* 43, 321-340, 2009.
- [32] Batra RC, Zhang GM, SSPH basis functions for meshless methods, and comparison of solutions with strong and weak formulations, *Comput Mech* 41, 527-545, 2008.
- [33] Tsai CL, Guan YL, Batra RC, Ohanehi DC, Dillard JG, Nicoli E, Dillard DA, Comparison of the performance of SSPH and MLS basis functions for two-dimensional linear elastostatics problems including quasistatic crack propagation, *Comput Mech* 51, 19-34, 2013.
- [34] Tsai CL, Guan YL, Ohanehi DC, Dillard JG, Dillard DA, Batra RC, Analysis of cohesive failure in adhesively bonded joints with the SSPH meshless method, *International Journal of Adhesion & Adhesives*, 51, 67-80, 2014.

- [35] Karamanli A, Mugan A, Solutions of two-dimensional heat transfer problems by using symmetric smoothed particle hydrodynamics method, *Journal of Applied and Computational Mathematics* 1, 1-6, 2012.
- [36] Karamanli A, Bending Deflection Analysis of a Semi-Trailer Chassis by Using Symmetric Smoothed Particle Hydrodynamics, *International Journal of Engineering Technologies*, 1, 4, 134-140, 2015.
- [37] Karamanli A, Mugan A, Strong form meshless implementation of Taylor series method, *Appl. Math. Comput.* 219, 9069-9080, 2013 .
- [38] Karamanli A, Different Implementation Approaches of the Strong Form Meshless Implementation of Taylor Series Method, *International Journal of Engineering Technologies*, Vol. 1, No:3, 2015.
- [39] Kaewumpai, S., Luadsong, A., Two-field-variable meshless method based on moving kriging interpolation for solving simply supported thin plates under various loads. *J. King Saud Univ. Sci.*, 1018–3647, 2014.
- [40] Yimnak, K., Luadsong, A., A local integral equation formulation based on moving kriging interpolation for solving coupled nonlinear reaction–diffusion equations. *Adv. Math. Phys.*, 2014.
- [41] Zhuang, X., Zhu, H., Augarde, C., The meshless Shepard and least squares (MSLS) method, *Comput Mech*, 53, 343-357, 2014.
- [42] Fatahi, H., Nadjafi, JS, Shivanian, E, New spectral meshless radial point interpolation (SMRPI) method for the two-dimensional Fredholm integral equations on general domains with error analysis, [Journal of Computational and Applied Mathematics](#), 264, 196-209, 2016.